Optimized Contact Geometries for High Speed Disconnect Switches

Gyu Cheol Lim¹, T. Damle², L. Graber²
¹Seoul National University, Seoul, Korea
²Georgia Institute of Technology, Atlanta, USA

Abstract—Fast mechanical disconnect switches are an integral part of hybrid circuit breakers, which are proposed as protection devices to clear faults in medium voltage distribution systems. Compared to their conventional counterparts, hybrid circuit breakers can have the ability to limit the fault current, which could allow more interconnections between substations with advantages with respect to grid reliability and resiliency. Furthermore, they enable the integration of distributed generation such as small solar power installations without expensive changes to the grid infrastructure. The proposed design of an ultrafast mechanical disconnect switch operates in vacuum, carries continuous current similar to conventional vacuum interrupters, opens at current zero, features minimum moving mass, and has an open contact separation of less than a millimeter. The limited separation distance requires an optimized contact geometry to keep the electric field within safe limits, minimize the moving mass, and reduce contact resistance. This paper proposes different contact geometries and uses finite element analysis to compare the contact geometries with respect to maximum electric field, mass, and contact resistance. Reductions of mass by 50% and reduction of contact resistance of 10% have been achieved.

Keywords—electrical contact, Bruce profile, Rogowski profile, contact resistance.

I. INTRODUCTION

Hybrid circuit breakers, a device that combines solid state switches with an ultrafast disconnect switch (UFDS), are increasingly often proposed as protection devices for medium voltage alternating current (MVAC) and medium voltage direct current (MVDC) distribution systems. Applications include micro grids and shipboard power systems of all electric ships [1-2]. Depending on the design, they can limit the fault current by their high-speed characteristics, which makes them a potential solution to ever increasing fault current levels in distribution systems in densely populated cities [3]. While most of the work on hybrid circuit breakers has focused on different power electronic circuits [4] with the goal to limit the fault current and its operation in tandem with a fast mechanical disconnector [5], work on the details of the UFDS is rather limited and focuses on two variants: the Thompson coil principle [6] and piezoelectric actuators [7]. The great advantage of submillisecond switching time of UFDS often comes at the cost of limited contact seperation between open contacts, often in the order of less than a millimeter when a piezoelectric actuator is used. The resulting high electric field could lead to electrical breakdown between

the open contacts and any local field enhancement caused by the geometery of the contacts must be minimized. Furthermore, electric contacts must be made of materials with high critical breakdown field, have smooth surfaces and feature a geometry that minimises the electric field. This paper compares electrical contacts with different surface geometries with respect to maximum electric field. Since the contact geometries also affect the mass of the contacts and the resistance between them when closed, these factors are also compared. Considerations with respect to the cost structure of contact material and manufacturing have not been considered in this study. UFDS are currently a research project and only prototypes have been designed and built. Future work will need to take into consideration material costs and manufacturing aspects.

Comparative analysis on electric field and resistance has been conducted for different contact geometries: Spherical, Elliptical, Bruce, and Rogowski contacts. Bruce and Rogowski profiles are well known uniform field electrode profiles, which have been adopted to be used as contact geometries. Electric field distribution for contact separation of 0.5 mm were modeled in finite elements to compare the peak electric field of the different contact designs. The choice of 0.5 mm contact separation is based on the design of an existing disconnect switch [7]. The contact diameter was also varied over a range of 2 mm to 10 mm. Moreover, the electric resistance of each contact is analyzed and compared to understand the expected tradeoffs between minimum field enhancement and minimum contact resistance.

II. CONTACT GEOMETRIES DESIGN

For contact modeling and simulation, different geometries of the contact are proposed. A spherical contact geometry is selected as a common basis of comparison among the three other contacts: elliptical, Rogowski, and Bruce contacts. Unlike spherical contacts, the other three proposed contact geometries have at least two variable parameters that define the slope and height of the contacts. The relationship between height and radius for each contact will be discussion in Section IV.

A. Design of Spherical Contacts

Conventional spherical contact can be modeled by rotating a quarter of a circle, $-\pi/2 \le \theta \le 0$ with the center as the rotation of axis.

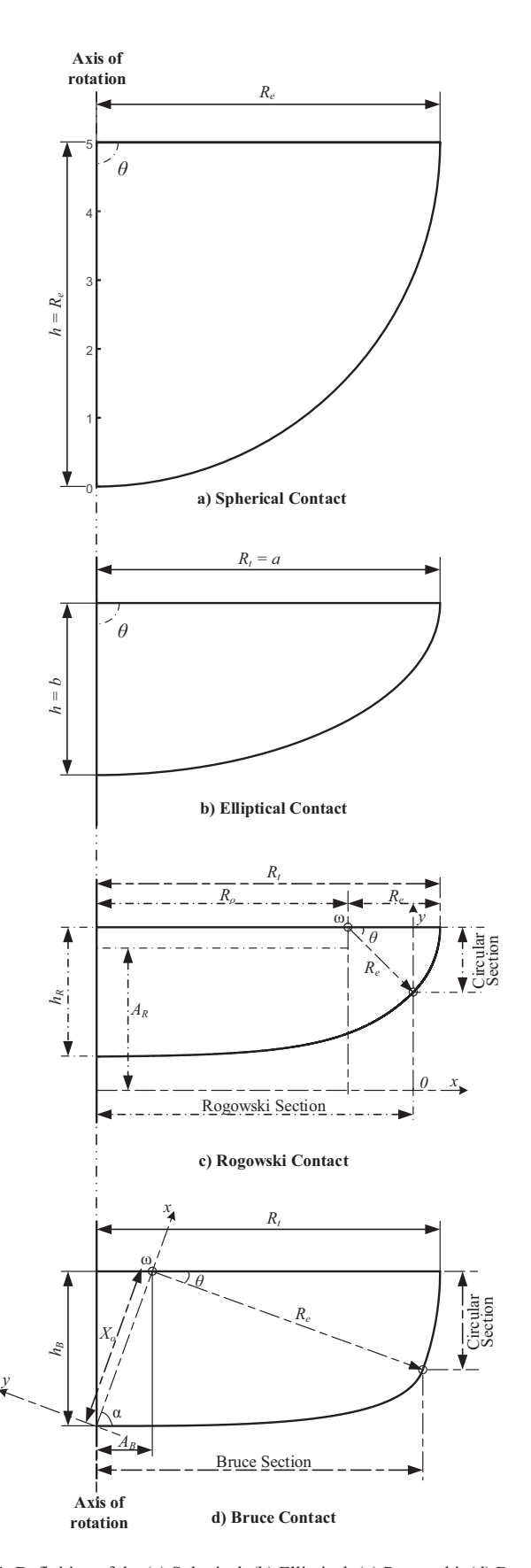


Fig. 1. Definition of the (a) Spherical, (b) Elliptical, (c) Rogowski, (d) Bruce Contacts [9, 10]

$$\begin{cases} x_{S} = R_{e} \cdot \cos \theta + x_{\omega} \\ y_{S} = R_{e} \cdot \sin \theta + y_{\omega} \end{cases}$$
 (1)

Spherical contacts are defined by only one variable, the radius R_e . The height is subsequently equal to the value of the radius. Here x_ω and y_ω are the center coordinate of spherical contact.

B. Design of Elliptical Contact

To have more design variables for the contact geometry, elliptical contacts are considered. Elliptical contacts have two variables, a, and b which determine the radius and the height respectively. The contact is modeled by rotating a quarter of the ellipse, $-\pi/2 \le \theta \le 0$.

$$\begin{cases} x_E = a \cdot \cos \theta + x_{\omega} \\ y_E = b \cdot \sin \theta + y_{\omega} \end{cases}$$
 (2)

One of the biggest advantages of elliptical profiles is the ability to adjust the height of the contact since it is an independent parameter (Fig. 1(b)). This allows to reduce the mass of the contact and the contact resistance.

C. Design of Rogowski Contact

The Rogowski electrode profile is defined by two different sections: the exponential (or: Rogowski) section and the circular section [8, 9]. In this paper, to make a contact model from a Rogowski profile, the exponential section and a partial circular section are adopted. Starting from the exponential Rogowski curve, it continues as a circular curve until its slope becomes vertical at the edge of the contact.

The Rogowski section of the contact is defined as follows:

$$\begin{cases} x_R = \frac{A_R}{\pi} \left(\phi + e^{\phi} \cos \psi \right) \\ y_R = \frac{A_R}{\pi} \left(\psi + e^{\phi} \sin \psi \right) \end{cases}$$
 (3)

In the equation (3), Ψ is the equipotential surface, ϕ is the line of force, and A is the characteristic distance separating the plane electrode from the infinite ground plane [8]. For modeling the contact, the parameter A is determined based on the radius of contact R_t , Ψ , and ϕ :

$$A_{R} = \frac{\pi \cdot R_{t}}{\frac{1 + \cos \psi}{\sin \psi} \sqrt{2(1 + \cos \psi)} \left(\left| \phi_{\min} \right| + e^{\phi_{\max}} \cos \psi - 1 \right)}$$
(4)

The transition between the Rogowski and the circular section is taken at $\phi = 0$ [8].

The circular section is defined as follows:

$$\begin{cases} x_c = R_e \cdot \cos \theta + x_\omega \\ y_c = R_e \cdot \sin \theta + y_\omega \end{cases}$$
 (5)

Where the center coordinate of the circular section is at (x_{ω}, y_{ω}) . To assure a smooth transition between the Rogowski and

the circular sections of the contact, the coordinate of the center should be [8]:

$$x_{\omega} = -\frac{A_{R}}{\pi}$$

$$y_{\omega} = \frac{A_{R}}{\pi} \left[\frac{(1 + \cos\psi)^{2}}{\sin\psi} + \sin\psi + \psi \right]$$
(6)

Along with the center coordinate, it is necessary to specify the point to start the circular section from the Rogowski section. The transition coordinate happens at $(0, y_o)$, where y_o can be defined as:

$$y_o = \frac{A_R}{\pi} (\psi + \sin \psi) \tag{7}$$

As described above, the end point of the circular section is at the location where the slope becomes vertical. From the starting point of the circular section to the last position, the angle is defined as $\theta = \beta$ and the range of θ is $0 \le \theta \le \beta$, where β , the angle between, is determined by:

$$\beta = -\sin^{-1} \left(\frac{y_{\omega} - y_{o}}{R_{e}} \right) \tag{8}$$

The total radius of the Rogowski contact is the sum of the corresponding radius of the circular section and the Rogowski section.

$$R_t = R_a + R_a \tag{9}$$

Where

$$R_{e} = \frac{A_{R}}{\pi} \cdot \frac{1 + \cos\psi}{\sin\psi} \sqrt{2(1 + \cos\psi)}$$

$$R_{o} = \frac{A_{R}}{\pi} \cdot \left(\phi_{\min} + e^{\phi_{\min}} \cos\psi - 1\right)$$
(10)

The conventional Rogowski profile corresponds to the equipotential surface of $\Psi = \pi/2$. Since Ψ is a predetermined value, the Rogowski profile is defined by the parameters of radius, R_t , and line of force, ϕ . The value of ϕ determines the curvature of the contact which contributes to the height. The angle $|\phi|$ must be big enough to avoid a tip at the center, which

would enhance the electric field and increase the contact resistance. Since Rogowski curve is an exponential function, the slope converges to 0 as $|\phi|$ increases. The minimum $|\phi|$ value is when the slope of the Rogowski curve approaches near zero and the electric field enhancement becomes negligible at the center. As ϕ approach to negative infinity, the curve of the contact gets flatter, and the contact would become more like a cylindrical shape.

D. Design of Bruce Contact

The Bruce electrode profile consists of three different sections: plane, sinusoidal (Bruce), and circular section [8, 10]. In this paper, to make a contact model from a Bruce profile, the plane section is eliminated and only the sinusoidal section and a portion of the circular section are adopted. Starting from a sinusoidal curve, it converts to the circular curve until its slope becomes vertical. The Bruce section of the contact is defined as follows:

$$y_{B} = -R_{e} \sin\left(\frac{x}{X_{o}} \frac{\pi}{2}\right) \tag{11}$$

 X_o is the distance of the circular section center ω and R_e is the radius of the circular section. A_B is a radial distance beyond which the Bruce section extends before meeting the circular section. Here, α is the characteristic angle of the sinusoidal section [8].

$$X_o = \frac{A_B}{\cos \alpha} \tag{12-1}$$

$$R_e = \frac{2}{\pi} X_o \tan \alpha \tag{12-2}$$

 A_B is determined by the variable of total radius, R_t and angle, α as following:

$$A_B = \frac{R_t}{\frac{2}{\pi} \cdot \frac{\tan \alpha}{\cos \alpha} + 1} \tag{13}$$

Circular section is defined as follows:

$$\begin{cases} x_c = R_e \cdot \cos\theta + x_\omega \\ y_c = R_e \cdot \sin\theta + y_\omega \end{cases}$$
 (14)

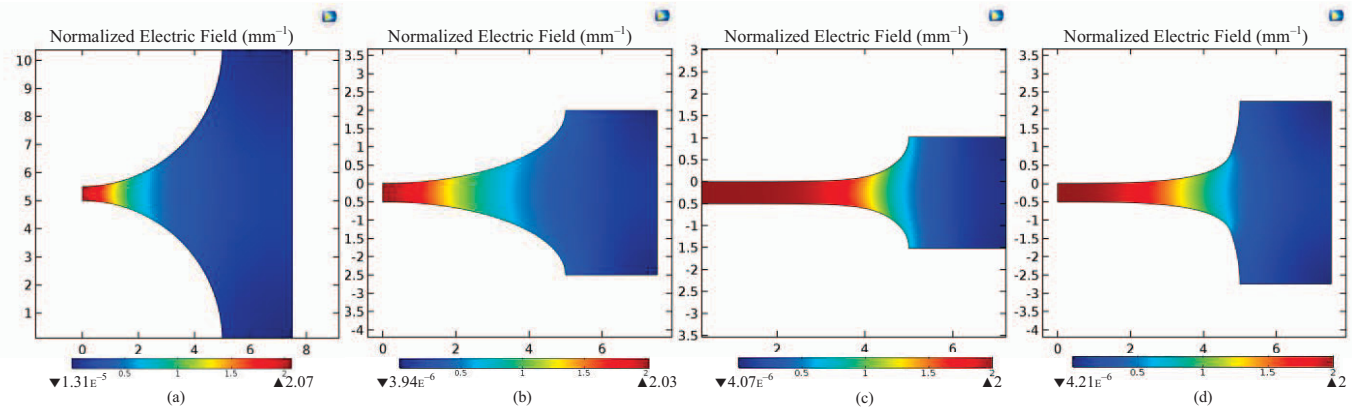


Fig. 2. FEM Result of Normalized Electric Field Distribution for 5 mm Radius $< R_t = 5$ mm> (a) Spherical, (b) Elliptical< h = 2mm>, (c) Rogowski $< |\phi| = 540$ >, and (d) Bruce $< \alpha = 70^\circ$ > Contact

Where the center coordinate of the circular section is at (x_{ω}, y_{ω}) .

$$x_{\omega} = X_{o}$$

$$y_{\omega} = 0$$
(15)

Started from the last point of the Bruce section, the angle of the circular section needs to be determined. The circular section stops when the slope of the section becomes vertical. Therefore, the angle between the circular section β , can be determined by (16). Where the rotating circular angle is $-\pi/2 \le \theta \le \beta$.

$$\beta = -\frac{\pi}{2} + \sin^{-1} \left(\frac{y_{\omega}^{\alpha} - y_{o}^{\alpha}}{R_{e}} \right) \tag{16}$$

The total radius of the Bruce contact is sum of the corresponding radius of the circular section and the radial direction of the Bruce section.

$$R_{t} = A_{B} + R_{e} \tag{17}$$

Bruce contacts have two variable parameters of radius R_e and angle α , the latter mainly determining the curvature of the contacts, which determines the height. The available range of α is from 0 to 90°. The curvature of the Bruce section gets flatter as either α decreases or increase from the point of 55.5°.

III. ELECTRIC FIELD ANALYSIS

The electric field in the test gap separation was modeled using a finite element model (FEM). In this simulation, the test gap for all contacts is set to be 0.5 mm. Varying both radius and design parameters for each contact geometry, the peak electric field is measured within the gap. The medium in the gap separation is considered vacuum. The bottom contact is grounded and the potential of the top contact is at 1 V. This allows to normalize the electric field, i.e. express it as a function of the geometry only, which results in a unit of [mm⁻¹]. Theoretically, a uniform electric field of a certain magnitude is produced within the space limited between two parallel plane electrodes of infinite dimensions separated by a distance d and subjected to a potential difference of U [2]. In the contact case, ideally a normalized electric field of 2 mm⁻¹ is expected as the minimum intensity of the field with the 0.5 mm gap.

$$E = U/d \tag{18}$$

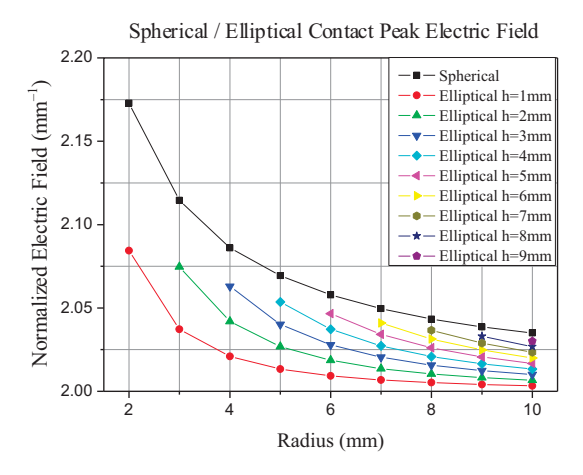
A. Electric Field Distribution for Spherical Contact

The normalized electric field distribution of a 5 mm radius spherical contact is shown in Fig. 2(a). The peak electric field is located at the center of the contact, and it is measured to be 2.075 mm⁻¹. For a radius of 2 mm to 10 mm, the peak electric field is measured within the set gap separation and it is shown in Fig. 3(a). As the radius of the contact becomes bigger, the reduction of electric field is observed.

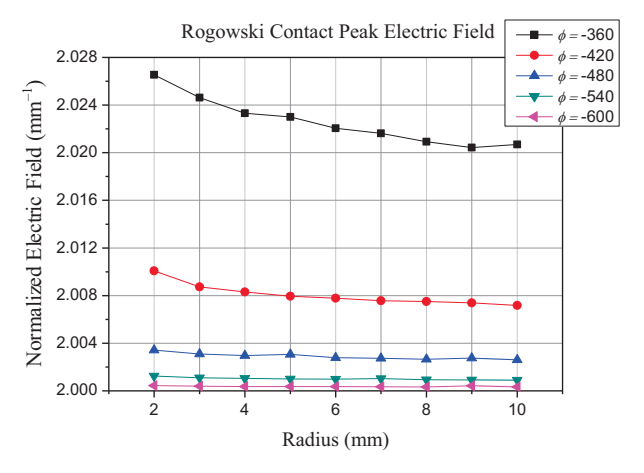
B. Electric Field Distribution for Elliptical Contact

The electric field for the case of elliptical contacts is simulated for a radius of 2 mm to 10 mm, and heights of less

than the corresponding radius. The measured peak electric fields for different heights are shown in Fig. 3(a). The comparison between spherical and elliptical contact is visually shown and it is noticeable that the peak electric field of elliptical contacts always lie below the field of spherical contact. With a smaller height than that of the spherical contact, the elliptical contacts can achieve a smaller peak



(a) Spherical and Elliptical Contact



(b) Rogowski Contact

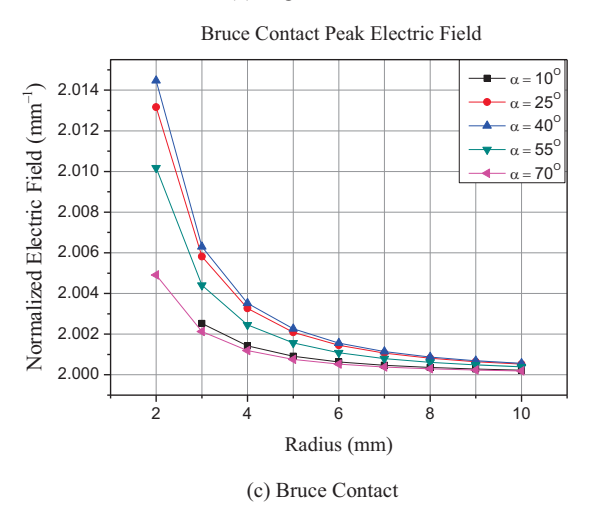


Fig. 3. Peak Electric Field of Contacts with Various Radius and Parameters

TABLE I PEAK ELECTRIC FIELD OF CONTACTS

Radius = 5mm	
Contact Geometry	Normalized Electric Field
-	
Spherical	2.07 [mm ⁻¹]
Elliptical $(h = 1)$	2.01 [mm ⁻¹]
Rogowski ($\phi = -540$)	2.00 [mm ⁻¹]
Bruce (α = 55°)	2.00 [mm ⁻¹]

Peak Electric Field of Contacts

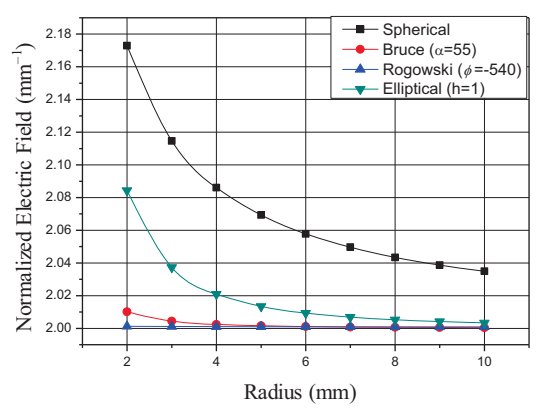


Fig. 4. Overall Comparative Electric Field between Contact Geometries electric field. The difference is more apparent when the radius and the height are small.

C. Electric Field Distribution for Rogowski Contact

Fig. 2(b) represents the electric field distribution model for Rogowski contacts with a radius of 5 mm and ϕ of -540. A more concentrated electric field distribution is observed since the surface became flatter than the spherical contact. As the value of $|\phi|$ increases, the Rogowski contact becomes flatter and the height of contact also decreases. In this simulation, the dynamic change of the peak electric field ϕ is observed to be within -300 to -600. As shown in Fig. 3(b), the peak electric field converges to 2 mm⁻¹ as $|\phi|$ increases and the difference among the electric field becomes smaller. The magnitude is significantly lower than the peak electric field of the spherical contact.

D. Electric Field Distribution for Bruce Contact

Fig. 2(c) shows the FEM electric field distribution model for Bruce contact with radius of 5 mm and α of 70°. The peak electric field of Bruce contacts with a radius varying from 2 mm to 10 mm and various values of α is plotted in Fig. 3(c). The appearance of the plot is similar to that of spherical and elliptical contact. However, the magnitude of electric field is *smaller* than for Rogowski Contact.

The overall comparison of peak electric field among four different contact models is shown in Fig. 4. For the complete range of radius from 2 mm to 10 mm, the Rogowski and Bruce contacts represent minimum peak electric field with values close to 2 mm⁻¹. Spherical contacts, which are used as a basic comparative model, show a distinguishable difference of peak electric field compared to other models. Elliptical contacts have similar slope to spherical contact but a smaller value. The peak electric field values for contacts of 5 mm radius are listed in Table I. Rogowski and Bruce contacts result in a 3.3% smaller peak electric field than the spherical contact. The greater the radius of the contacts, the smaller die difference of electric field between Rogowski and Bruce profiles. All the contact models indicates that the peak electric field decreases as the radius increases.

IV. RESISTANCE ANALYSIS

From the electric field analysis result, the presented contact models other than spherical contact indicate that similar or lower peak electric field can be achieved with a reduced height of the contacts compared to that of spherical contacts. In this section, the resistance of each contact model is simulated. For the comparison of the contact resistance, a fixed radius of 5 mm and a fixed height of the contact models are used. Copper is used as the material in modelling. Spherical contacts cannot vary the height with a fixed radius. The height is chosen to be same for elliptical, Rogowski, and Bruce contacts. Subsequently, the resistance of the contacts are compared with congruent contact radius and height.

A. Height of Contacts

The radius of all contact profiles is set to 5 mm. This is also the height of the spherical contact profile. For all other contact profiles, the height needs to be determined. In case of elliptical

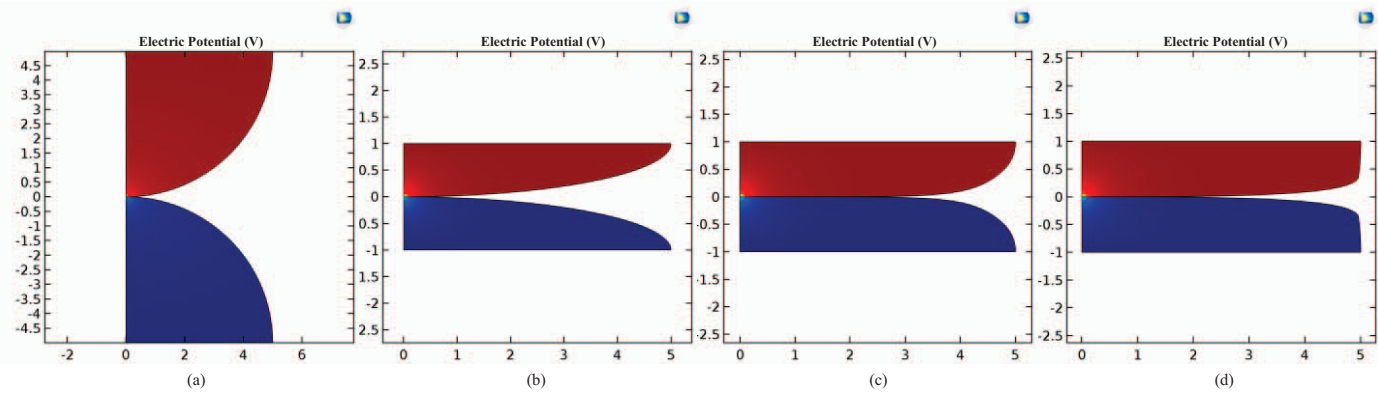


Fig. 5. FEM Result of Contact Resistance for (a) Spherical, (b) Elliptical, (c) Rogowski, and (d) Bruce Contact

TABLE II
RESISTANCE OF CONTACTS

Contact Geometry	Resistance
Spherical	147 [μΩ]
Elliptical	143 [μΩ]
Rogowski	137 [μΩ]
Bruce	132 [μΩ]

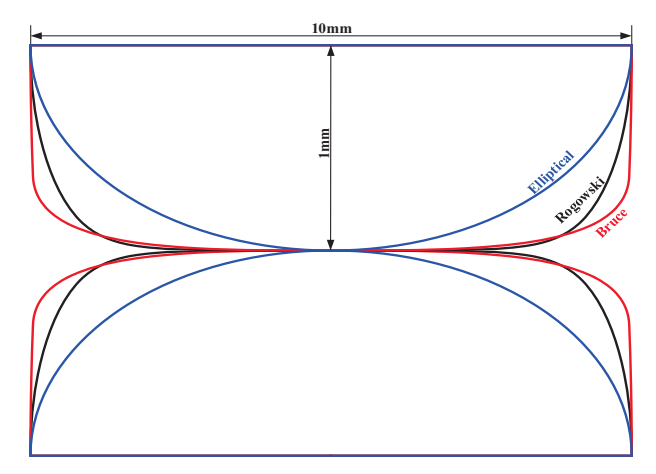


Fig. 6. Radius of 5 mm and Height of 1 mm Contact Models for Elliptical, Rogowski, Bruce Contacts (Vertical Axis Magnified)

contact, a height of 1 mm is chosen. By fixing the height of the contact to 1 mm for Rogowski and Bruce contacts, the parameter of ϕ for Rogowski and α for Bruce was determined. For Rogowski contacts, the height is defined by (19), where A_R is a function of radius and ϕ .

$$h_R = \frac{A_R}{\pi} \sin \psi \left(\cot^2 \frac{\psi}{2} + 1 + e^{\phi_{\min}} \right)$$
 (19)

For Bruce contacts, the height is defined by (20), where A_B is a function of radius and α .

$$h_B = A_B \tan \alpha \tag{20}$$

Using (19) and (20), the appropriate α and ϕ are derived. Rogowski contacts have a height of 1 mm and a radius of 5 mm when $\phi = -549.5$, and Bruce contacts have a height of 1 mm and the radius of 5 mm when $\alpha = 12.95^{\circ}$ or 82.48° . The curvatures of the contacts for designed height and radius is shown in Fig. 6.

B. Resistance of Contacts

The resistances of each contact geometry are determined using an FEM model by setting the contacts in touch. By setting one end as input terminal and the other end as ground terminal, the resistance is measured.

When contacts are in touch, ideally contacts touch in a single point. However, in practical cases, due to the slightly elastic nature of contact materials and the high contact pressure, multiple points or surface areas on the contacts touch. In this FEM model, the touching area of the contacts is set to be 0.01 mm². Fig. 5 represents the simulation setup and result of the contact resistance model for the discussed contact

profiles. Resistances for each contact are listed in the Table II. It is noted that the resistance of spherical contacts is the highest, followed by elliptical, Rogowski, and Bruce contact profiles. Bruce contacts result in a 10% smaller contact resistance than the spherical contact.

V. CONCLUSION

Modeling contacts from the electrode profiles has shown advantages over the conventional spherical contacts. The proposed geometries of Rogowski, Bruce, and elliptical contacts show a reduced field enhancement in the submillimeter separation range, which is important for applications with limited contact travel such piezoelectrically actuated disconnect switches. These contact profiles also have a significantly reduced height compared to spherical contacts, which results in a reduction of bulk contact resistance and mass. These optimized contact geometries are expected to substantially improve the performance of high speed disconnect switches. Long term performance of the proposed contact geometries needs to be investigated.

ACKNOWLEDGMENT

The authors would like to thank M. Steurer from the Center of Advanced Power Systems (CAPS), Florida State University, for his expert advice and great discussions. This work has been supported in part by the NSF grant #1700887.

REFERENCES

- E. Bowles, E. Ortiz, J. Zgliczynski, "Magnetically Pulsed DC Hybrid Circuit Breaker for the Next Generation Integrated Power System (NGIPS)," *Electric Machines Technologies Symposium (EMTS)*, San Diego CA, 2008.
- [2] E. Hebner, "DC Protection," Electric Ship Research and Development Consortium for the Office of Naval Research, 2011.
- [3] L. Graber, T. Lawrence, C. Widener, "NSF I-Corps Final Project Report," NSF Award 1547045, March 2016. https://www.nsf.gov/awardsearch/showAward?AWD ID=1547045
- [4] A. Shukla, G. D. Demetriades, "A survey on hybrid circuit-breaker topologies," *IEEE Transactions on Power Delivery*, 30(2), 627-641, 2015
- [5] M. Steurer, K. Fröhlich, W. Holaus, K. Kaltenegger, "A novel hybrid current-limiting circuit breaker for medium voltage: principle and test results", *IEEE transactions on power delivery*, 18(2), 460-467, 2003.
- [6] C. Peng, I. Husain, A.Q. Huang, "Evaluation of design variables in Thompson coil based operating mechanisms for ultra-fast opening in hybrid AC and DC circuit breakers", *IEEE Applied Power Electronics Conference and Exposition (APEC)*, pp 2325-2332, Mar. 2015
- [7] L. Graber, S. Smith, D. Soto, I. Novak, J. Owens, M. Steurer, "A new class of high speed disconnect switch based on piezo electric actuators", *IEEE Electric Ship Technologies Symposium (ESTS)*, pp 307-312, Jun. 2015
- [8] N. G. Trinh, "Electrode Design for Testing in Uniform Field Gaps," in *IEEE Transactions on Power Apparatus and Systems*, vol. PAS-99, no. 3, pp. 1235-1242, May 1980.
- [9] W. Rogowski, "Die elektrische Festigkeit am Rande des Plattenkondensators. Ein Beitrag zur Theorie der Funkenstrecken um Durchführungen", Archiv für Electrotechnik, Vol. 12, No. 1, 1923, pp. 1
- [10] F.M. Bruce, "Calibration of uniform-field spark-gaps for high-voltage measurement at power frequencies", Journal of IEE, Vol. 94, Part II, 1947, pp. 138-149.